

Adaptive double-phase ROF model: report on 2D experiments (continued)

Wojciech Górný* Michał Łasica† Alexandros Matsoukas‡

September 30, 2025

Abstract

This is the second part of the note which reports the results of several numerical experiments involving the adaptive double-phase ROF model in the two-dimensional case.

1 The girlface 512×512

Experiment 1.0.1.

1. $a = 60, b = 1200;$
2. $\alpha_h = 0.01;$
3. $\sigma = 0.01, 0.04;$
4. Tolerance level: $10^{-4};$

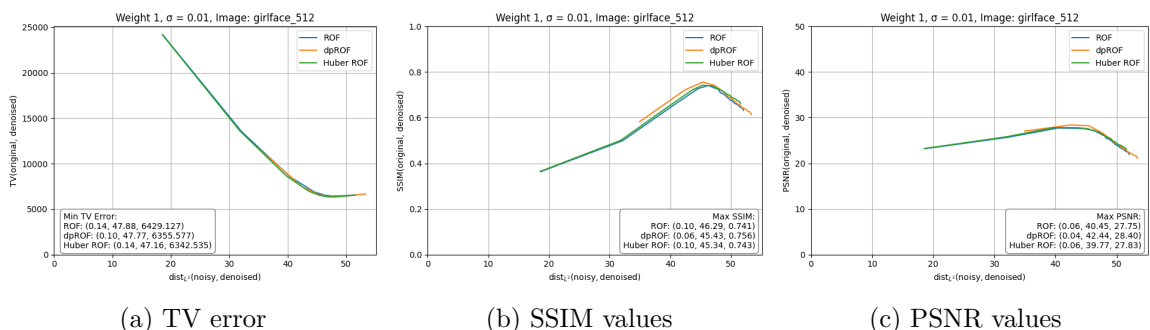


Figure 1: Plots of the metrics with respect to L^2 -distance from the noisy image, for classical ROF, double-phase ROF and Huber ROF ($a_h = 0.01$) with noise level $\sigma = 0.01$.

*Faculty of Mathematics, Universität Wien, Oskar-Morgerstern-Platz 1, 1090 Vienna, Austria; Faculty of Mathematics, Informatics and Mechanics, University of Warsaw, Banacha 2, 02-097 Warsaw, Poland; wojciech.gorny@univie.ac.at

†Institute of Mathematics of the Polish Academy of Sciences, Śniadeckich 8, 00-656 Warsaw, Poland; mglasica@impan.pl

‡Department of Mathematics, School of Applied Mathematical and Physical Sciences, National Technical University of Athens, Zografou Campus, 157 80 Athens, Greece; alex.matsoukas@mail.ntua.gr

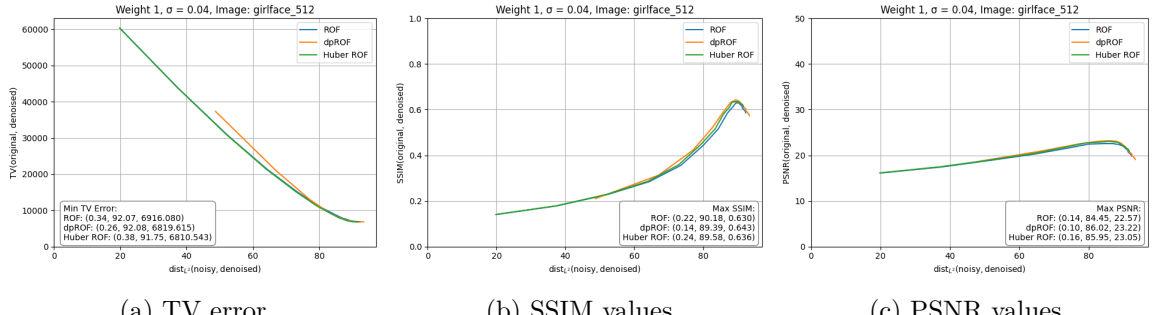


Figure 2: Plots of the metrics with respect to L^2 -distance from the noisy image, for classical ROF, double-phase ROF and Huber ROF ($a_h = 0.01$) with noise level $\sigma = 0.04$.

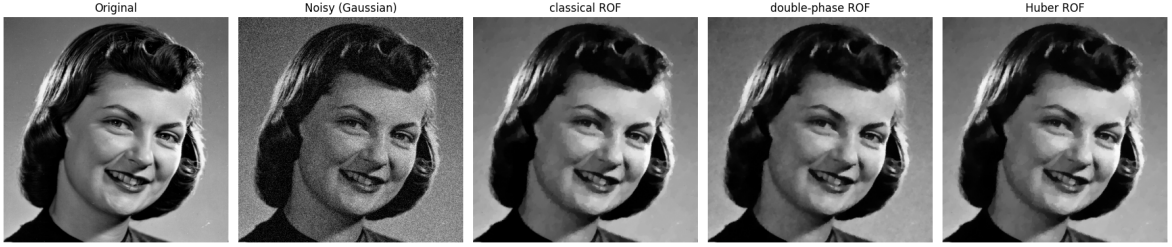
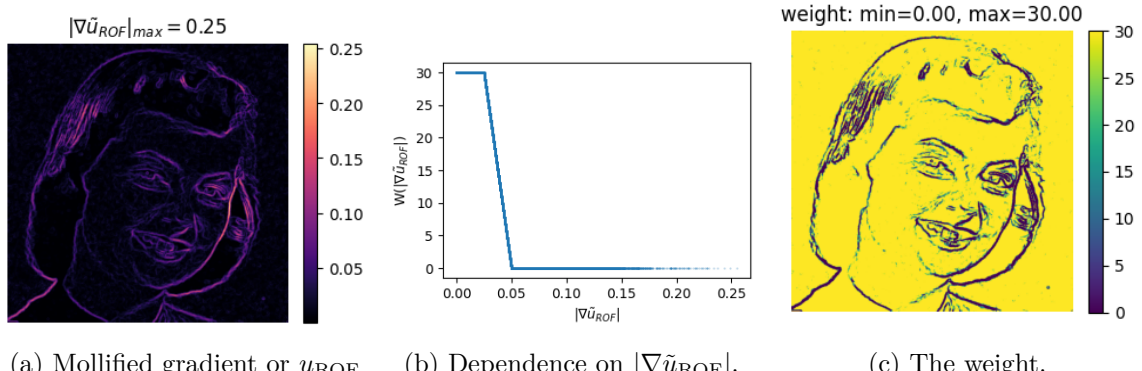


Figure 3: Original and noisy images of girlface, along with the denoised results corresponding to the maximum SSIM values. The methods shown are: classical ROF ($\lambda = 0.10$), double-phase ROF ($\lambda = 0.06$), and Huber ROF ($\alpha_h = 0.01$, $\lambda = 0.1$) with $\sigma = 0.01$.



Table 1: Evaluation of performance

error $\epsilon = 10^{-4}$	Classical ROF	Double-phase ROF	Huber ROF
λ	0.10	0.06	0.10
dist_{L^2}	46.29	45.43	45.39
maxSSIM	0.741	0.756	0.743
iterations	796	450 (+470)	1462
time	20.62s	28.47s (+15.98s)	38.67s



(a) Mollified gradient or u_{ROF}

(b) Dependence on $|\nabla \tilde{u}_{\text{ROF}}|$.

(c) The weight.

Figure 4: Construction of the weight from mollified gradient of u_{ROF} with $\lambda = 0.06$.

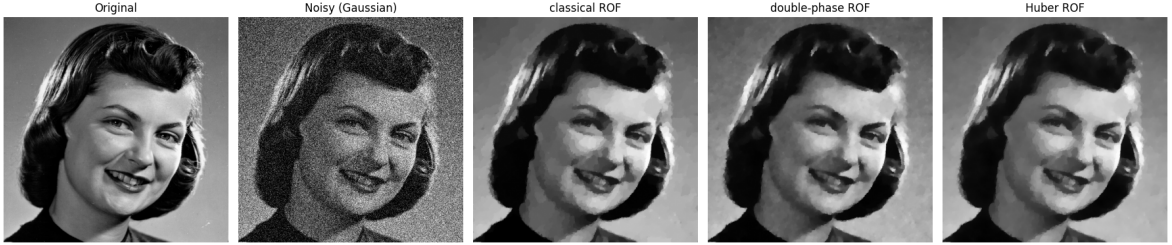


Figure 5: Original and noisy images of girlface, along with the denoised results corresponding to the maximum SSIM values. The methods shown are: classical ROF ($\lambda = 0.22$), double-phase ROF ($\lambda = 0.14$), and Huber ROF ($\alpha_h = 0.01$, $\lambda = 0.24$) with $\sigma = 0.04$.



Table 2: Evaluation of performance

error $\epsilon = 10^{-4}$	Classical ROF	Double-phase ROF	Huber ROF
λ	0.22	0.14	0.24
dist_{L^2}	90.18	89.39	89.58
maxSSIM	0.630	0.643	0.636
iterations	1192	675 (+762)	1835
time	32.55s	44.63s (+20.73s)	48.31s

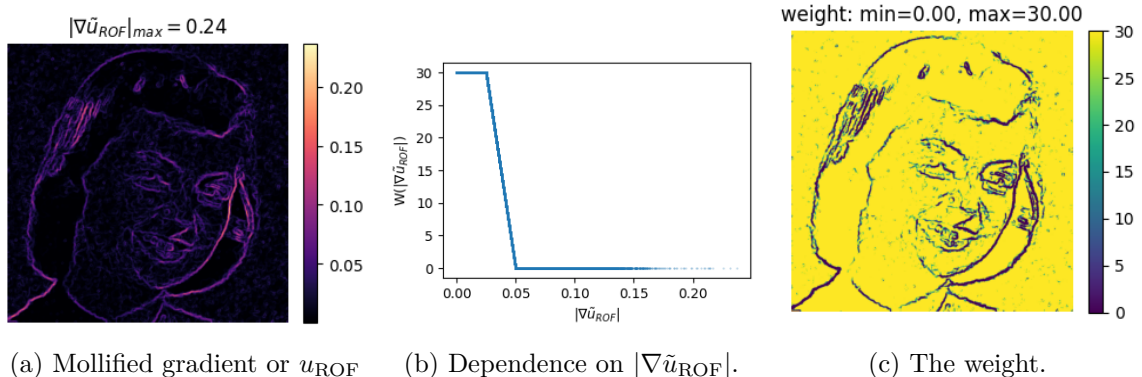


Figure 6: Construction of the weight from mollified gradient of u_{ROF} with $\lambda = 0.14$.

Experiment 1.0.2.

1. $a = 60, b = 1500$;
2. $\alpha_h = 0.01$;
3. $\sigma = 0.01, 0.04, 0.07$;
4. Tolerance level: 10^{-4} ;

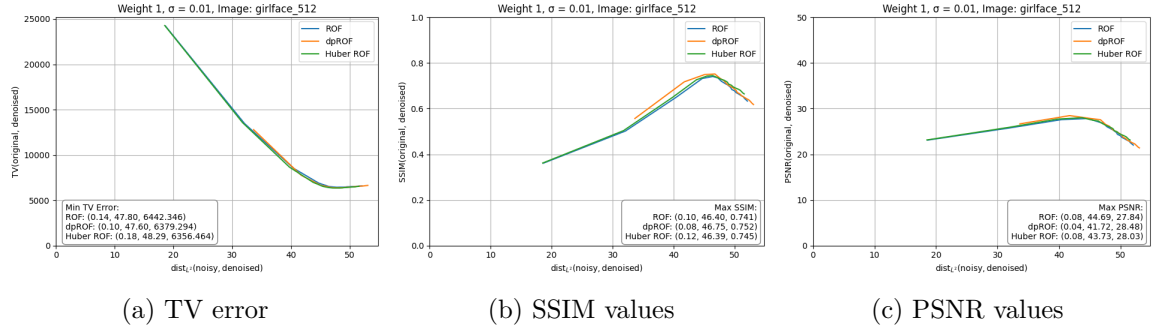


Figure 7: Plots of the metrics with respect to L^2 -distance from the noisy image, for classical ROF, double-phase ROF and Huber ROF ($a_h = 0.01$) with noise level $\sigma = 0.01$.

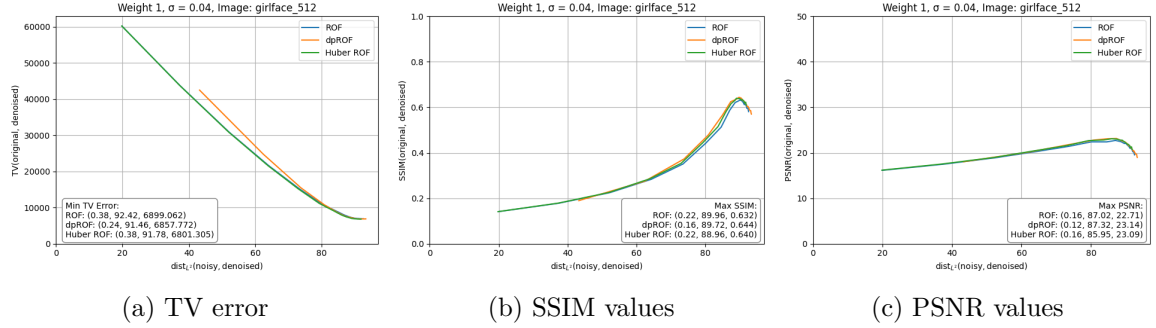


Figure 8: Plots of the metrics with respect to L^2 -distance from the noisy image, for classical ROF, double-phase ROF and Huber ROF ($a_h = 0.01$) with noise level $\sigma = 0.04$.

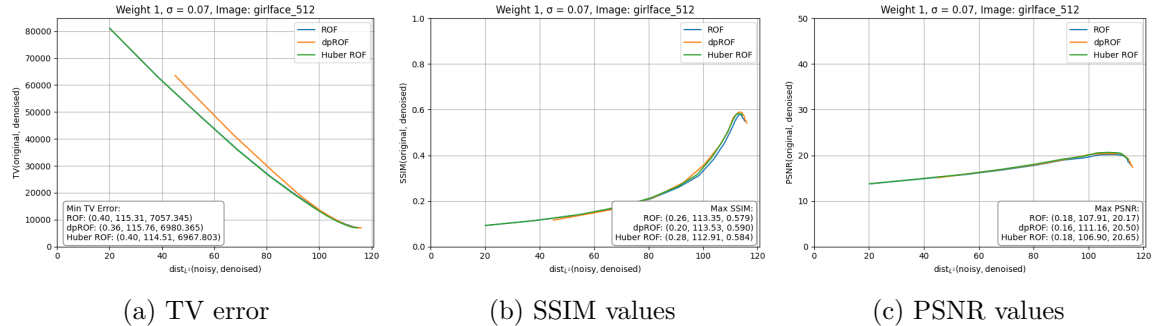


Figure 9: Plots of the metrics with respect to L^2 -distance from the noisy image, for classical ROF, double-phase ROF and Huber ROF ($a_h = 0.01$) with noise level $\sigma = 0.07$.

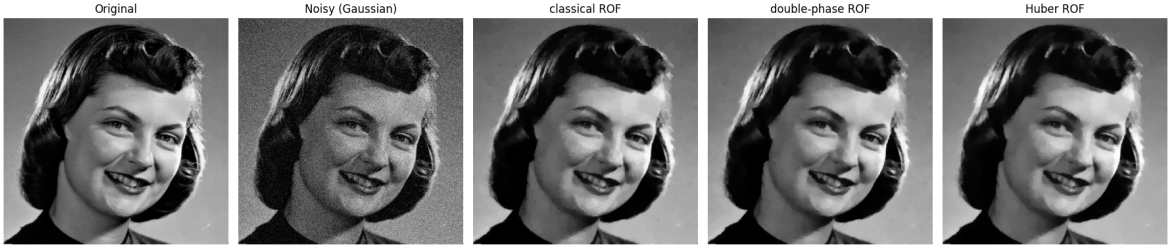
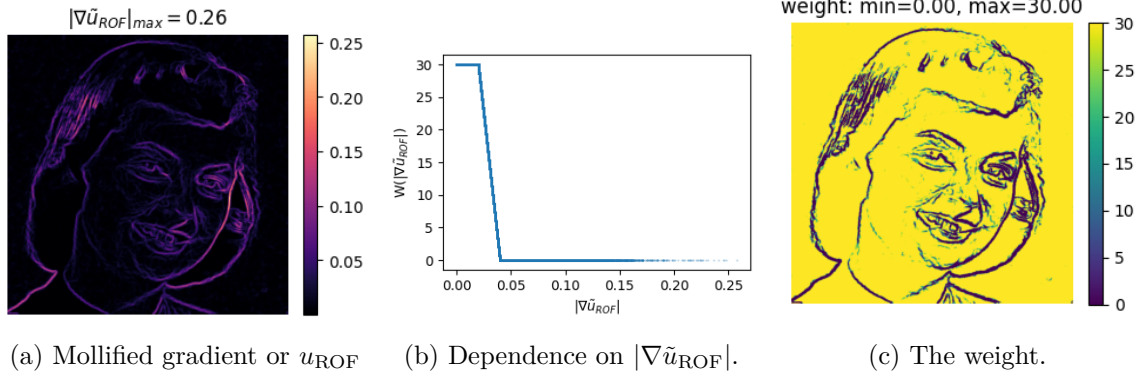


Figure 10: Original and noisy images of girlface, along with the denoised results corresponding to the maximum SSIM values. The methods shown are: classical ROF ($\lambda = 0.10$), double-phase ROF ($\lambda = 0.08$), and Huber ROF ($\alpha_h = 0.01$, $\lambda = 0.12$) with $\sigma = 0.01$.



Table 3: Evaluation of performance

error $\epsilon = 10^{-4}$	Classical ROF	Double-phase ROF	Huber ROF
λ	0.10	0.08	0.12
$dist_{L^2}$	46.40	46.75	46.39
maxSSIM	0.741	0.752	0.745
iterations	808	615 (+700)	1611
time	25.30s	42.37s (+19.19s)	41.33s



(a) Mollified gradient or u_{ROF} (b) Dependence on $|\nabla \tilde{u}_{\text{ROF}}|$. (c) The weight.

Figure 11: Construction of the weight from mollified gradient of u_{ROF} with $\lambda = 0.08$.

Experiment 1.0.3.

1. $a = 50, b = 1000$;
2. $\alpha_h = 0.005, 0.01$;
3. $\sigma = 0.01, 0.04, 0.07$;
4. Tolerance level: 10^{-4} ;

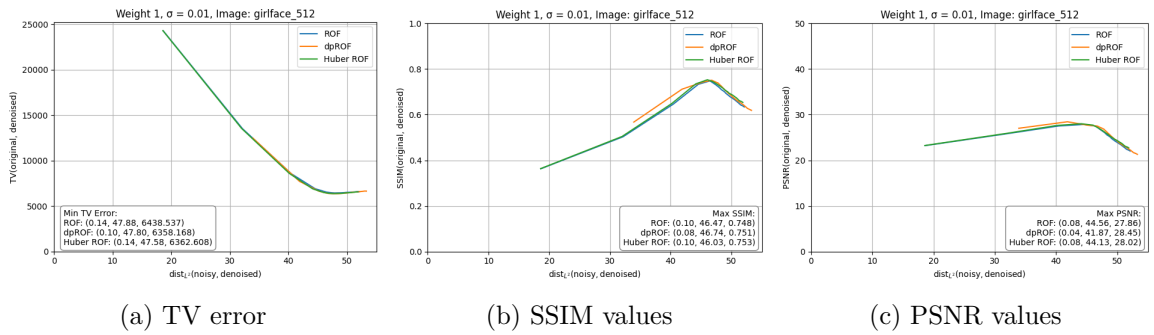


Figure 12: Plots of the metrics with respect to L^2 -distance from the noisy image, for classical ROF, double-phase ROF and Huber ROF ($\alpha_h = 0.005$) with $\sigma = 0.01$.

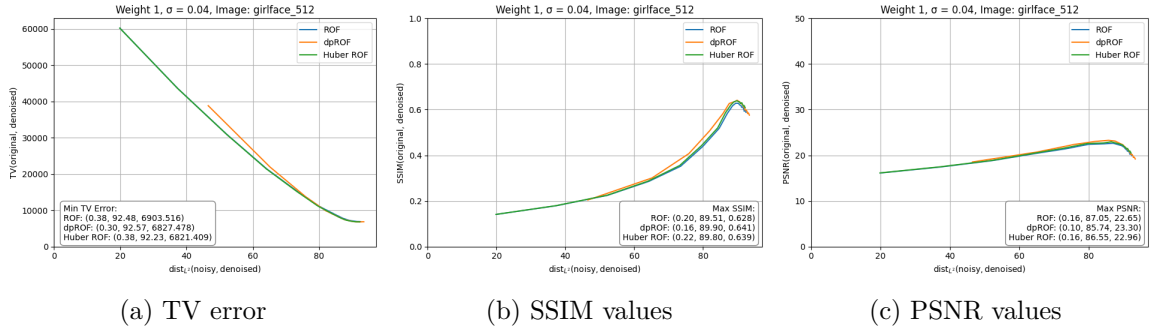


Figure 13: Plots of the metrics with respect to L^2 -distance from the noisy image, for classical ROF, double-phase ROF and Huber ROF ($\alpha_h = 0.005$) with $\sigma = 0.04$.

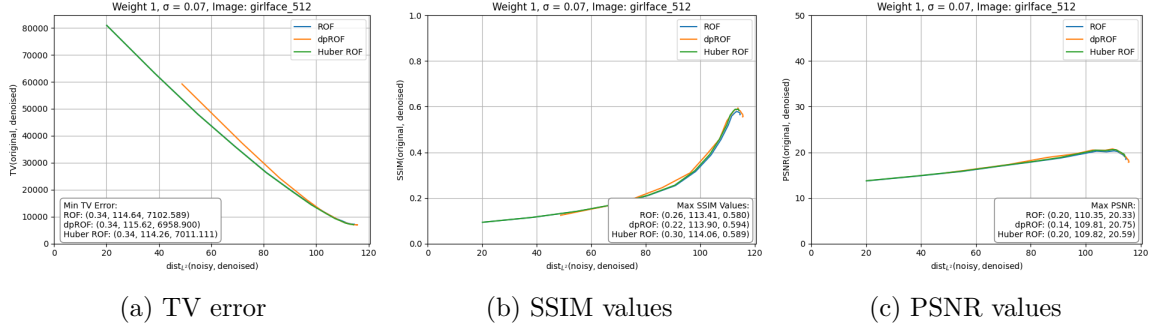


Figure 14: Plots of the metrics with respect to L^2 -distance from the noisy image, for classical ROF, double-phase ROF and Huber ROF ($\alpha = 0.005$) with $\sigma = 0.07$.

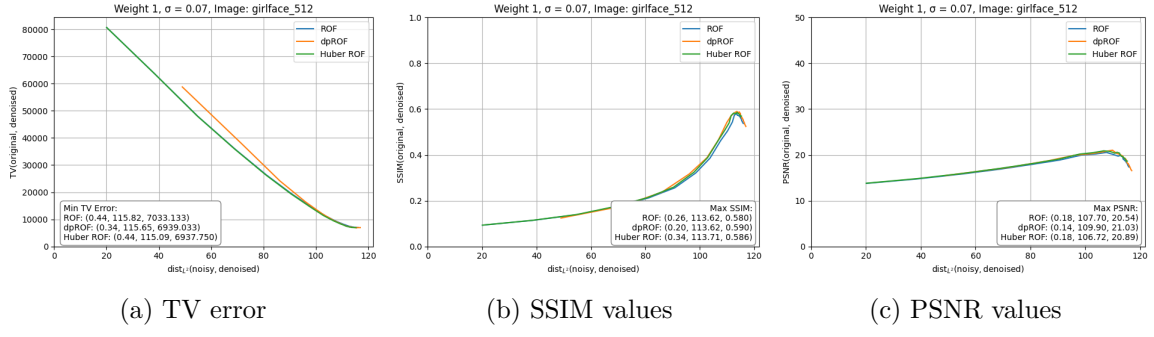


Figure 15: Plots of the metrics with respect to L^2 -distance from the noisy image, for classical ROF, double-phase ROF and Huber ROF ($\alpha = 0.01$) with $\sigma = 0.07$.

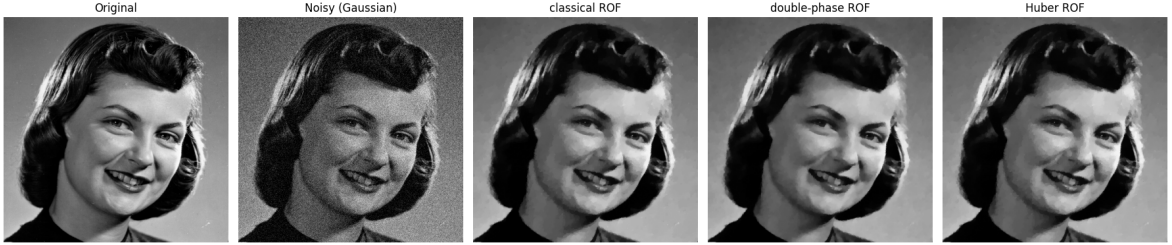
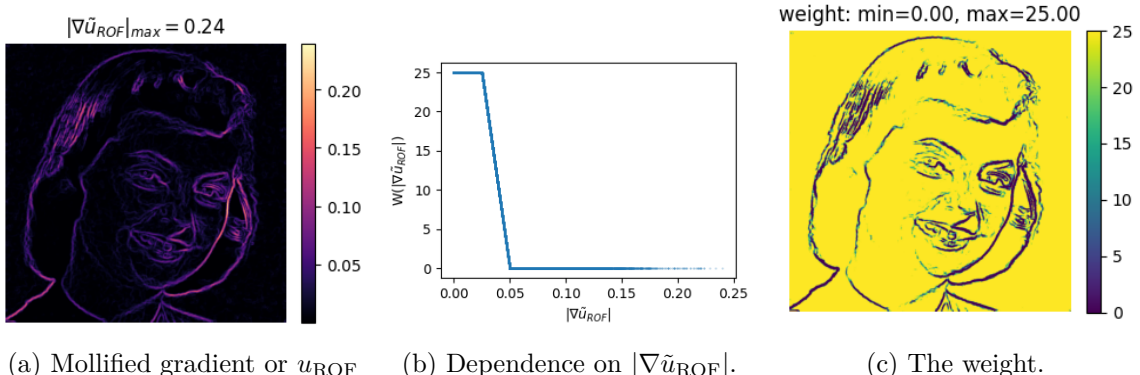


Figure 16: Original and noisy images of girlface, along with the denoised results corresponding to the maximum SSIM values. The methods shown are: classical ROF ($\lambda = 0.1$), double-phase ROF ($\lambda = 0.08$), and Huber ROF ($\alpha_h = 0.005$, $\lambda = 0.1$) with $\sigma = 0.01$.



Table 4: Evaluation of performance

error $\epsilon = 10^{-4}$	Classical ROF	Double-phase ROF	Huber ROF
λ	0.10	0.08	0.10
dist_{L^2}	46.47	46.74	46.03
maxSSIM	0.748	0.751	0.753
iterations	849	789 (+693)	1706
time	17.72s	21.06s (+19.31s)	46.27s



(a) Mollified gradient or u_{ROF} (b) Dependence on $|\nabla \tilde{u}_{\text{ROF}}|$. (c) The weight.

Figure 17: Construction of the weight from mollified gradient of u_{ROF} with $\lambda = 0.08$.

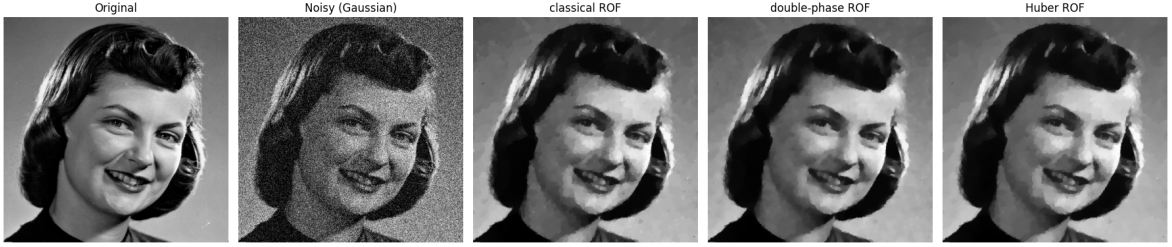


Figure 18: Original and noisy images of girlface, along with the denoised results corresponding to the maximum SSIM values. The methods shown are: classical ROF ($\lambda = 0.2$), double-phase ROF ($\lambda = 0.16$), and Huber ROF ($\alpha_h = 0.005$, $\lambda = 0.22$) with $\sigma = 0.04$.



Table 5: Evaluation of performance

error $\epsilon = 10^{-4}$	Classical ROF	Double-phase ROF	Huber ROF
λ	0.20	0.16	0.22
dist L^2	89.51	89.90	89.80
maxSSIM	0.628	0.641	0.639
iterations	1067	763 (+847)	2135
time	27.29s	52.80s (+22.84s)	62.95s

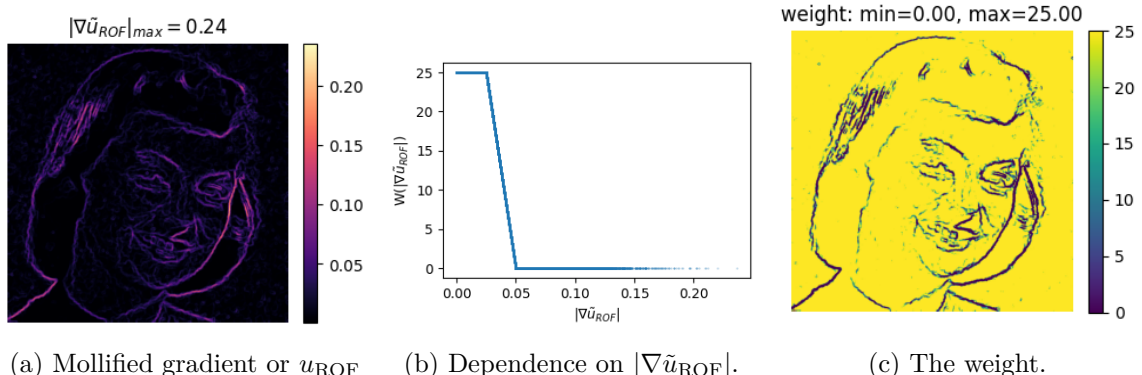


Figure 19: Construction of the weight from mollified gradient of u_{ROF} with $\lambda = 0.16$.

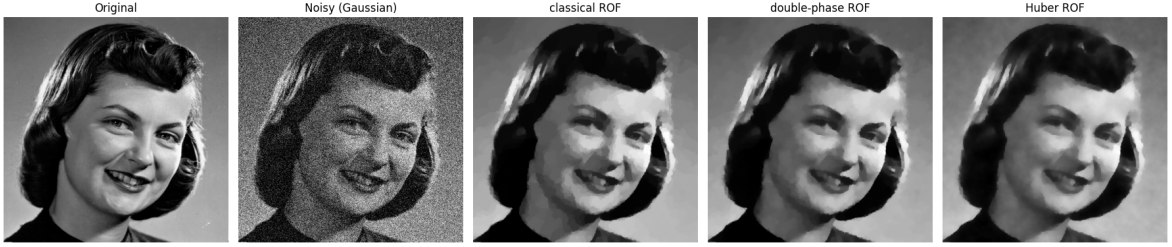
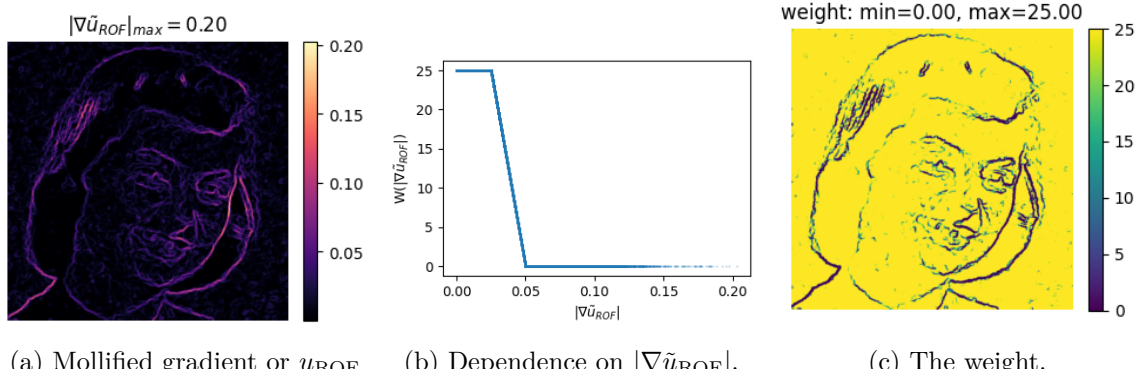


Figure 20: Original and noisy images of girlface, along with the denoised results corresponding to the maximum SSIM values. The methods shown are: classical ROF ($\lambda = 0.26$), double-phase ROF ($\lambda = 0.20$), and Huber ROF ($\alpha_h = 0.01, \lambda = 0.34$) with $\sigma = 0.07$.



Table 6: Evaluation of performance

error $\epsilon = 10^{-4}$	Classical ROF	Double-phase ROF	Huber ROF
λ	0.26	0.20	0.34
dist_{L^2}	113.62	113.62	113.71
maxSSIM	0.580	0.590	0.586
iterations	1334	951 (+970)	1710
time	30.13s	61.46s (+24.29s)	47.64s



(a) Mollified gradient or u_{ROF} (b) Dependence on $|\nabla \tilde{u}_{\text{ROF}}|$. (c) The weight.

Figure 21: Construction of the weight from mollified gradient of u_{ROF} with $\lambda = 0.20$.

2 Schnitzel 512×512

Experiment 2.0.1.

1. $a = 50, b = 1000$;
2. $\alpha_h = 0.01$;
3. $\sigma = 0.01, 0.04, 0.07$;
4. Tolerance level: 10^{-4} ;

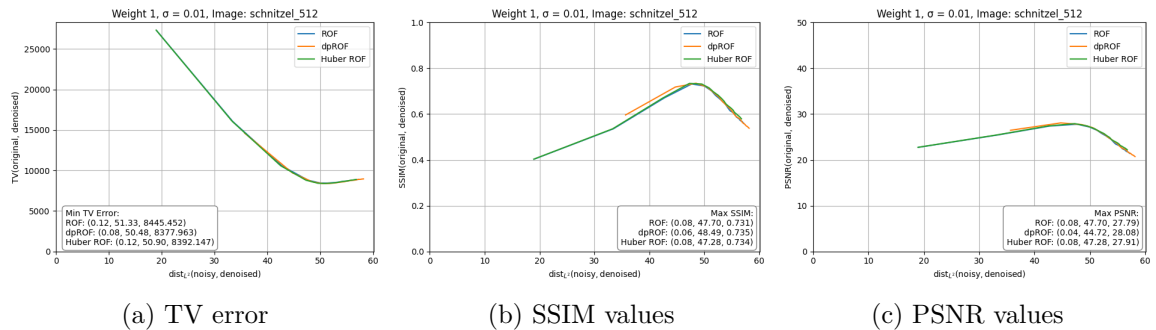


Figure 22: Plots of the metrics with respect to L^2 -distance from the noisy image, for classical ROF, double-phase ROF and Huber ROF ($a_h = 0.01$) with noise level $\sigma = 0.01$.

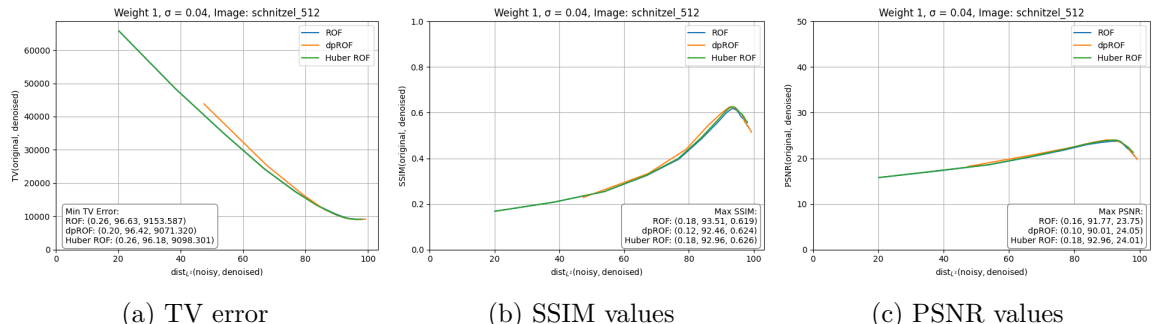


Figure 23: Plots of the metrics with respect to L^2 -distance from the noisy image, for classical ROF, double-phase ROF and Huber ROF ($a_h = 0.01$) with noise level $\sigma = 0.04$.

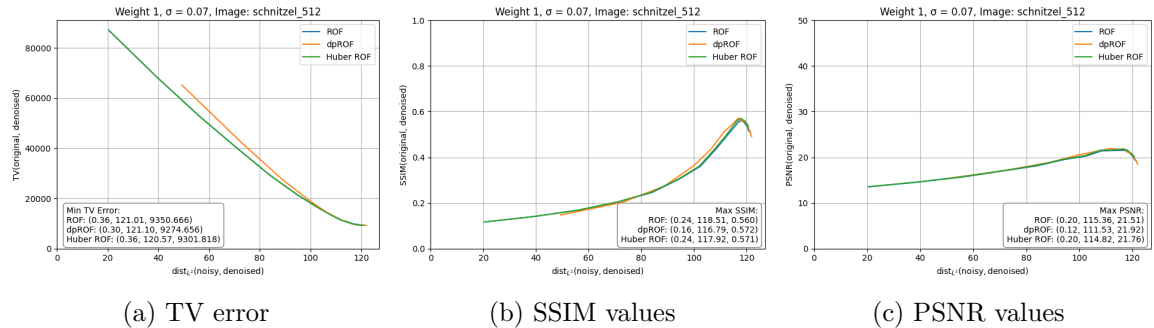


Figure 24: Plots of the metrics with respect to L^2 -distance from the noisy image, for classical ROF, double-phase ROF and Huber ROF ($a_h = 0.01$) with noise level $\sigma = 0.07$.



Figure 25: Original and noisy images of Schnitzel, along with the denoised results corresponding to the maximum SSIM values. The methods shown are: classical ROF ($\lambda = 0.08$), double-phase ROF ($\lambda = 0.06$), and Huber ROF ($\alpha_h = 0.01, \lambda = 0.08$) with $\sigma = 0.01$.

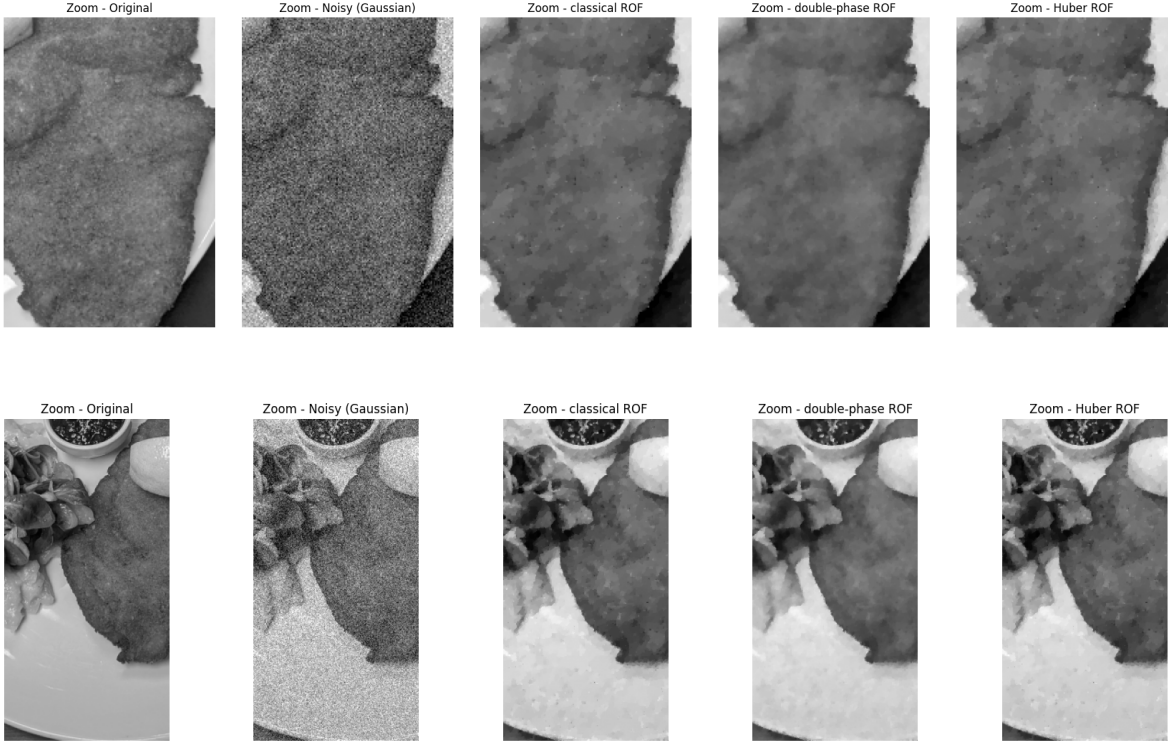


Table 7: Evaluation of performance

error $\epsilon = 10^{-4}$	Classical ROF	Double-phase ROF	Huber ROF
λ	0.08	0.06	0.08
dist L^2	47.70	48.49	47.28
maxSSIM	0.731	0.735	0.734
iterations	537	348 (+357)	1225
time	27.87s	33.30s (+13.22s)	46.17s

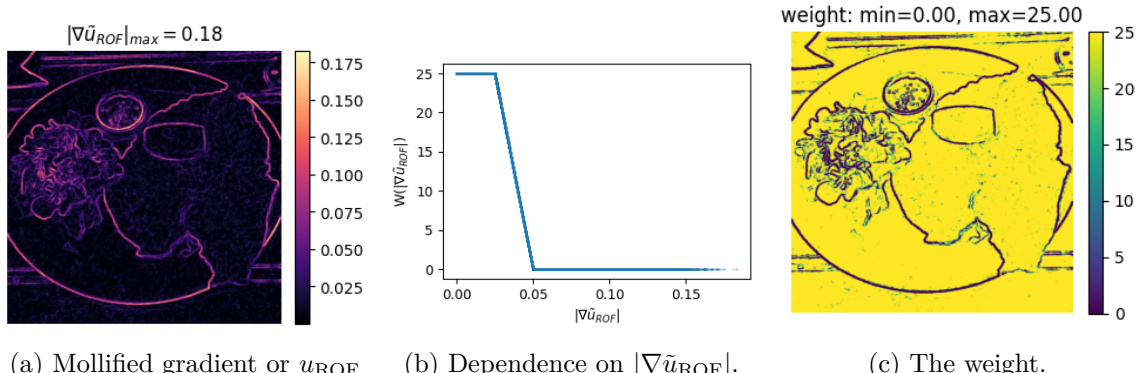


Figure 26: Construction of the weight from mollified gradient of u_{ROF} with $\lambda = 0.06$.

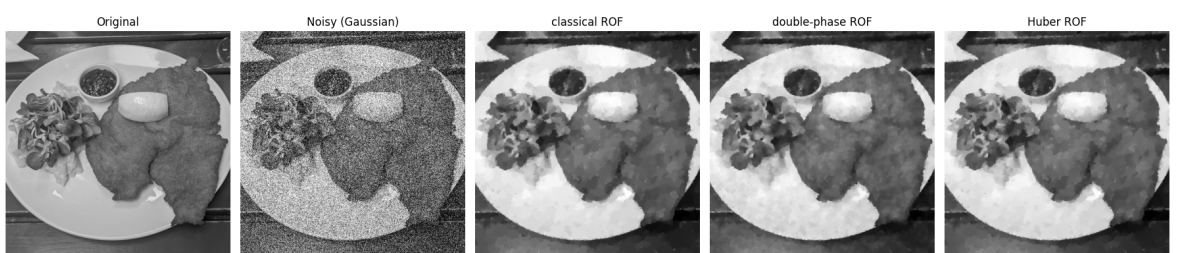


Figure 27: Original and noisy images of Schnitzel, along with the denoised results corresponding to the maximum SSIM values. The methods shown are: classical ROF ($\lambda = 0.24$), double-phase ROF ($\lambda = 0.16$), and Huber ROF ($\alpha_h = 0.01, \lambda = 0.24$) with $\sigma = 0.07$.

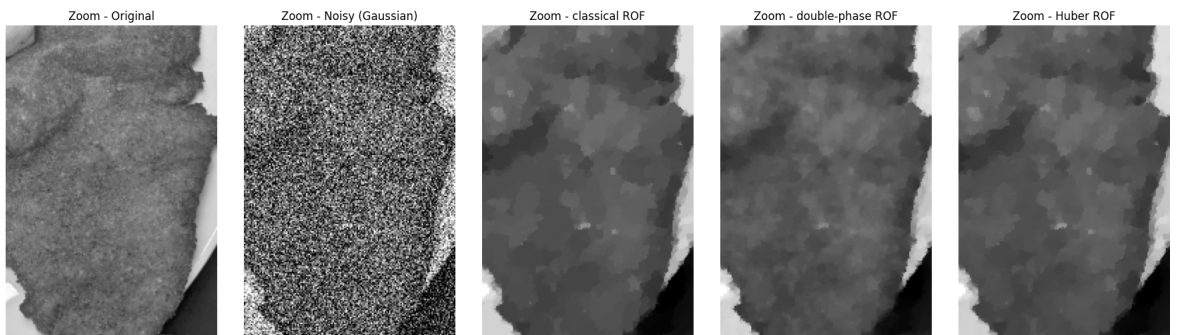


Table 8: Evaluation of performance

error $\epsilon = 10^{-4}$	Classical ROF	Double-phase ROF	Huber ROF
λ	0.24	0.16	0.24
dist _{L2}	118.51	116.79	117.92
maxSSIM	0.560	0.572	0.571
iterations	1009	559 (+602)	1789
time	31.77s	48.29s (+24.21s)	62.12s

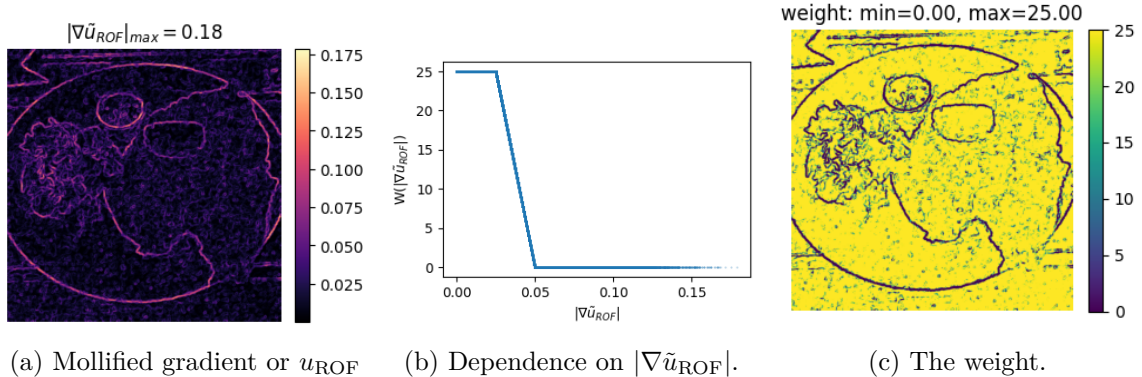


Figure 28: Construction of the weight from mollified gradient of u_{ROF} with $\lambda = 0.16$.

Experiment 2.0.2.

1. $a = 60, b = 1200$;
2. $\alpha_h = 0.01$;
3. $\sigma = 0.01, 0.04, 0.07$;
4. Tolerance level: 10^{-4} ;

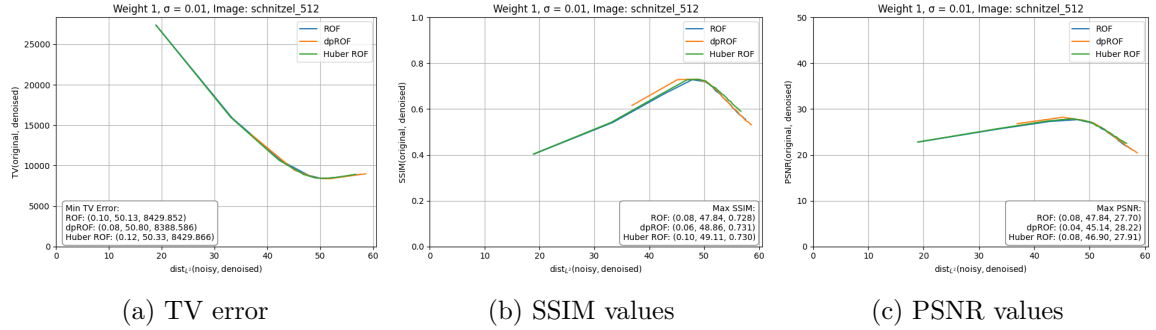


Figure 29: Plots of the metrics with respect to L^2 -distance from the noisy image, for classical ROF, double-phase ROF and Huber ROF ($a_h = 0.01$) with noise level $\sigma = 0.01$.

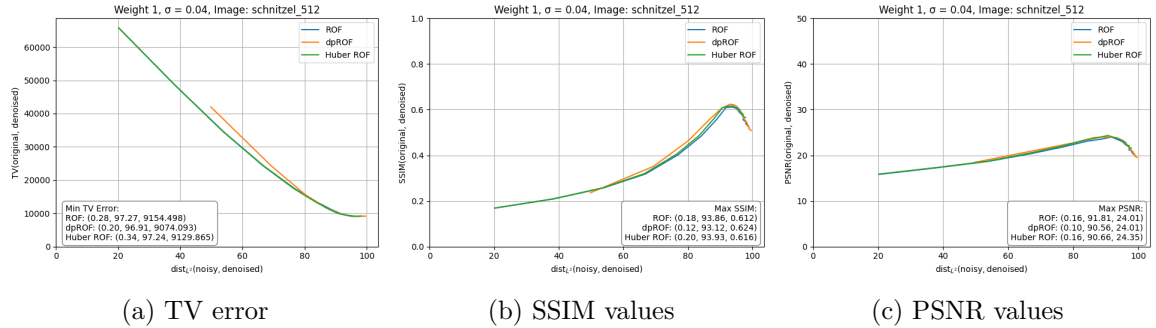


Figure 30: Plots of the metrics with respect to L^2 -distance from the noisy image, for classical ROF, double-phase ROF and Huber ROF ($a_h = 0.01$) with noise level $\sigma = 0.04$.

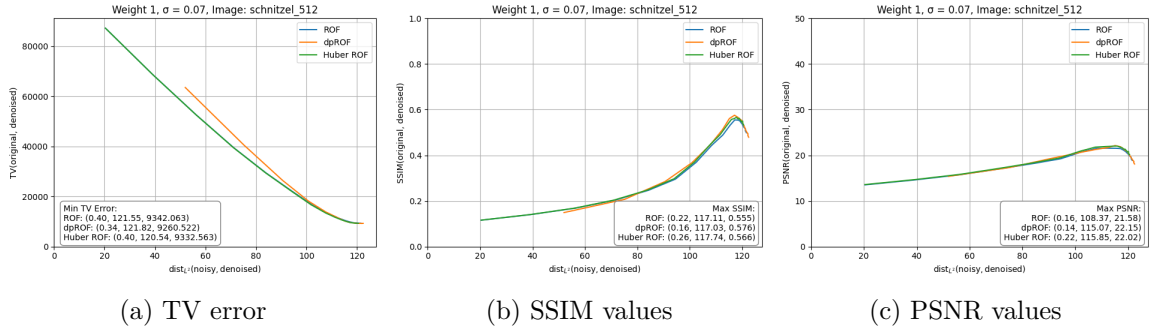


Figure 31: Plots of the metrics with respect to L^2 -distance from the noisy image, for classical ROF, double-phase ROF and Huber ROF ($a_h = 0.01$) with noise level $\sigma = 0.07$.

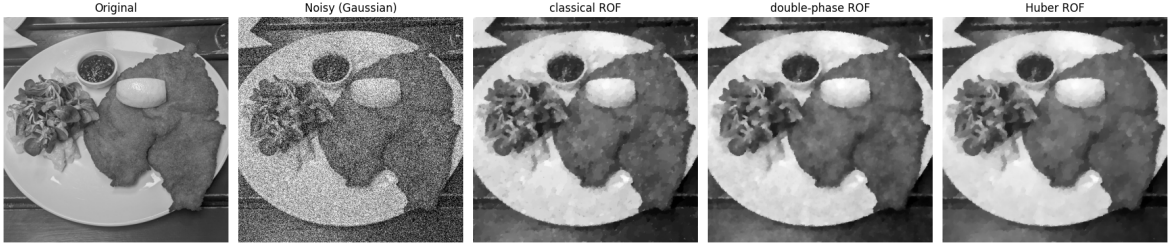


Figure 32: Original and noisy images of Schnitzel, along with the denoised results corresponding to the maximum SSIM values. The methods shown are: classical ROF ($\lambda = 0.22$), double-phase ROF ($\lambda = 0.16$), and Huber ROF ($\alpha_h = 0.01, \lambda = 0.26$) with $\sigma = 0.07$.

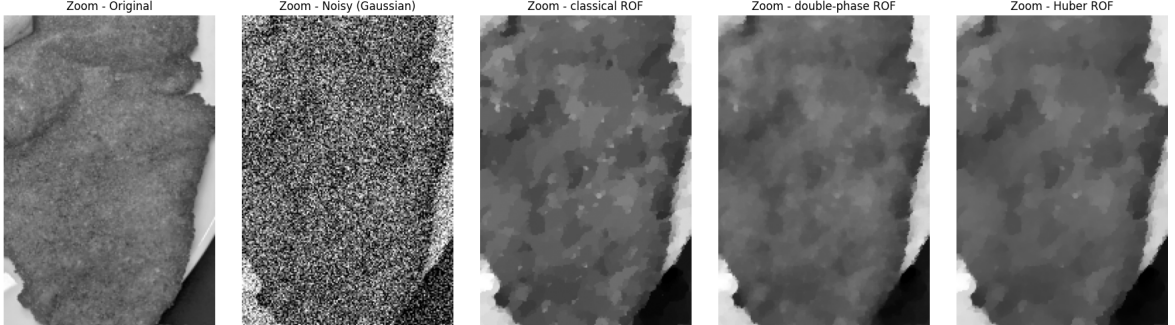


Table 9: Evaluation of performance

error $\epsilon = 10^{-4}$	Classical ROF	Double-phase ROF	Huber ROF
λ	0.22	0.16	0.26
dist $_{L^2}$	117.11	117.03	117.74
maxSSIM	0.555	0.576	0.566
iterations	833	552 (+587)	1880
time	22.42s	34.89s (+9.94s)	49.82s

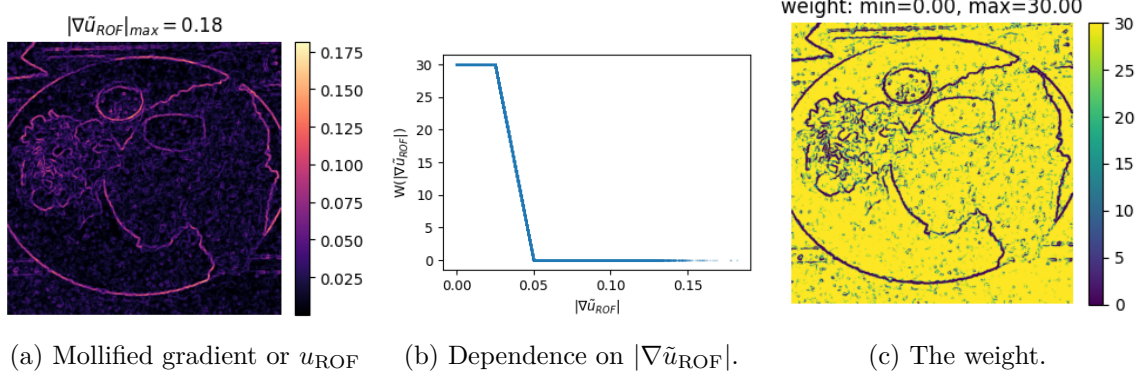


Figure 33: Construction of the weight from mollified gradient of u_{ROF} with $\lambda = 0.16$.

Experiment 2.0.3.

1. $a = 60, b = 1500$;
2. $\alpha_h = 0.01$;
3. $\sigma = 0.01, 0.04, 0.07$;
4. Tolerance level: 10^{-4} ;

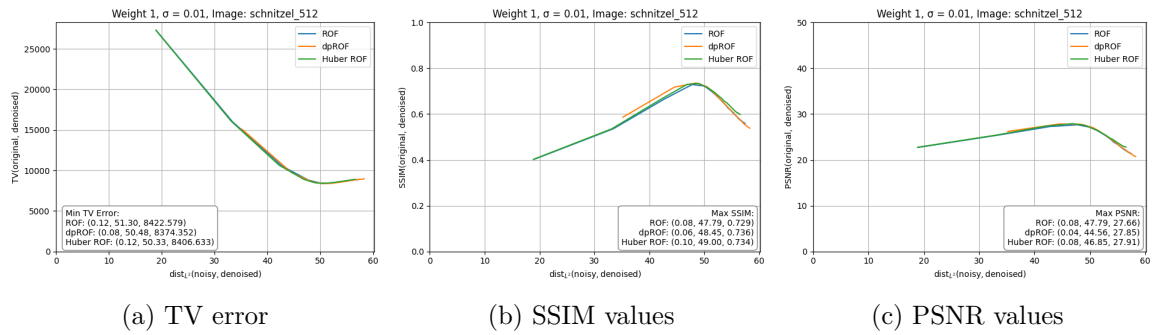


Figure 34: Plots of the metrics with respect to L^2 -distance from the noisy image, for classical ROF, double-phase ROF and Huber ROF ($a_h = 0.01$) with noise level $\sigma = 0.01$.

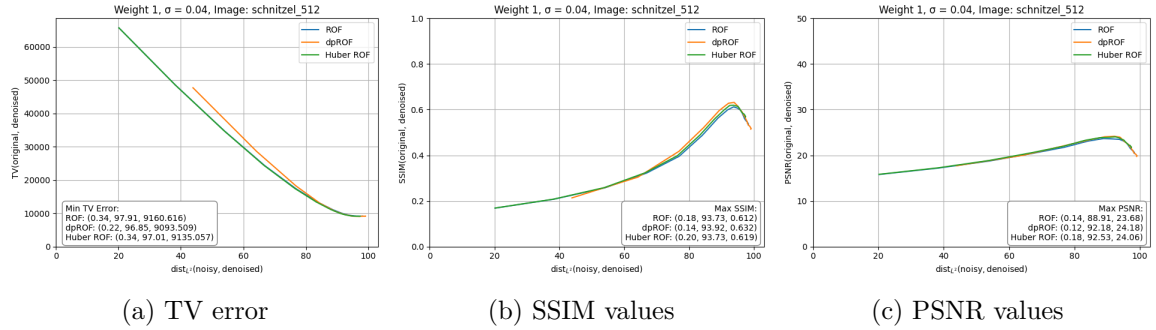


Figure 35: Plots of the metrics with respect to L^2 -distance from the noisy image, for classical ROF, double-phase ROF and Huber ROF ($a_h = 0.01$) with noise level $\sigma = 0.04$.

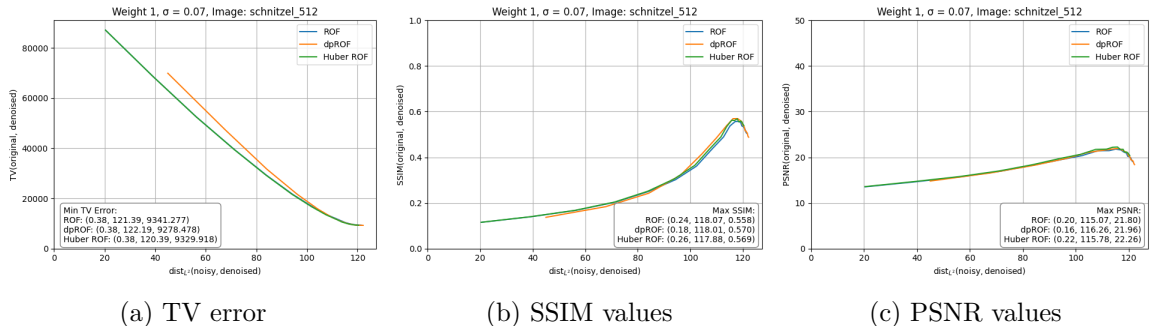


Figure 36: Plots of the metrics with respect to L^2 -distance from the noisy image, for classical ROF, double-phase ROF and Huber ROF ($a_h = 0.01$) with noise level $\sigma = 0.07$.

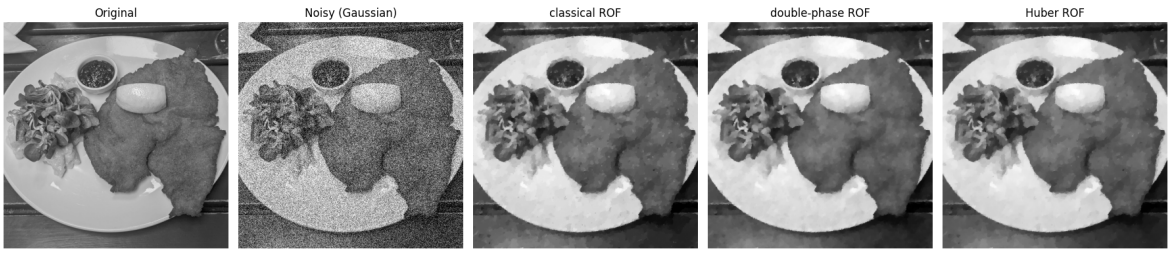


Figure 37: Original and noisy images of Schnitzel, along with the denoised results corresponding to the maximum SSIM values. The methods shown are: classical ROF ($\lambda = 0.18$), double-phase ROF ($\lambda = 0.14$), and Huber ROF ($\alpha_h = 0.01, \lambda = 0.20$) with $\sigma = 0.04$.

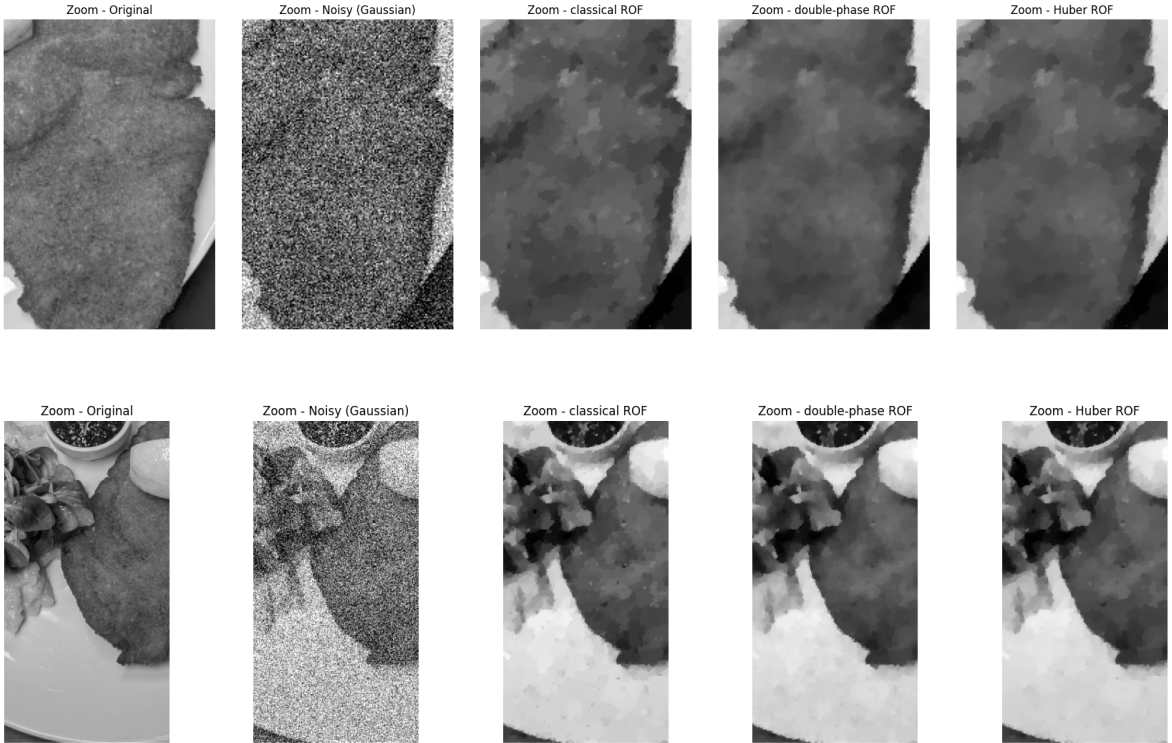


Table 10: Evaluation of performance

error $\epsilon = 10^{-4}$	Classical ROF	Double-phase ROF	Huber ROF
λ	0.18	0.14	0.20
dist_{L^2}	93.73	93.92	93.73
maxSSIM	0.612	0.632	0.619
iterations	821	576 (+623)	1740
time	28.53s	42.84s (+18.12s)	48.28s

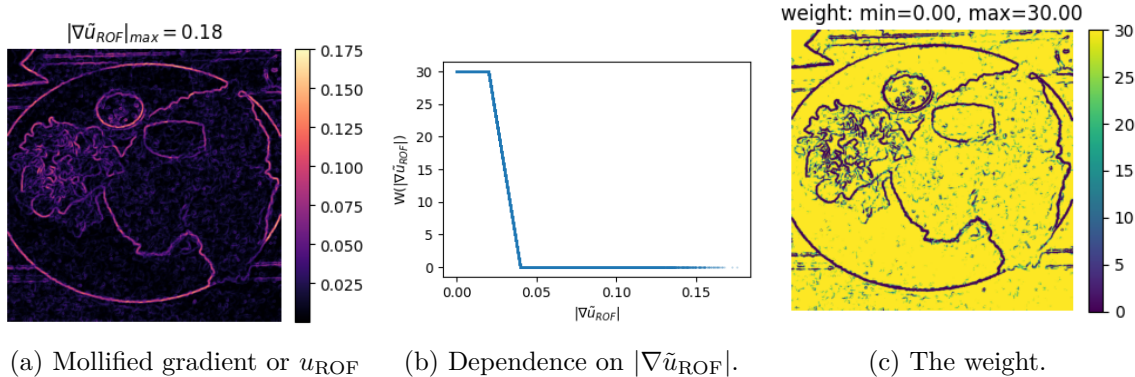


Figure 38: Construction of the weight from mollified gradient of u_{ROF} with $\lambda = 0.14$.

Acknowledgments. The work of the first author has been supported by the Austrian Science Fund (FWF), grants 10.55776/ESP88 and 10.55776/I5149. The second author has been partially supported by the grant 2024/55/D/ST1/03055 of the National Science Centre (NCN), Poland. The third author has been partially supported by the Special Account for Research Funding of the National Technical University of Athens.